

## Dynamic polaron tunneling in $\text{YBa}_2\text{Cu}_3\text{O}_7$ : Optical response and inelastic neutron scattering

M. I. Salkola and A. R. Bishop

*Theoretical Division, Los Alamos National Laboratory, Los Alamos, New Mexico 87545*

J. Mustre de Leon

*Applied Physics Department, Cinvestav Merida, Merida, Yucatan 97310, Mexico*

S. A. Trugman

*Theoretical Division, Los Alamos National Laboratory, Los Alamos, New Mexico 87545*

(Received 12 October 1993)

Coexisting electronic correlations and electron-phonon interactions have been proposed to lead to dynamic polaron-tunneling behavior for the axial oxygen in  $\text{YBa}_2\text{Cu}_3\text{O}_7$ . Emphasizing nonlinear and nonadiabatic effects, we show that this description leads to distinctive predictions consistent with structural, optical, and inelastic neutron-scattering data in the axial direction.

Much of the interpretation of lattice dynamics and optics in high- $T_c$  materials has relied on harmonic rigid-potential models. However, for certain structural features, recent studies indicate that aspects of the intrinsic dynamics in these systems may be highly nonlinear and nonadiabatic.

Here, we focus on the local dynamics of the axial oxygen O(4) and chain copper Cu(1) clusters—arranged as O(4)-Cu(1)-O(4) and located *between*  $\text{CuO}_2$  planes in  $\text{YBa}_2\text{Cu}_3\text{O}_7$ —and point out the basic signatures of a *polaron-tunneling* prediction<sup>1,2</sup> leading to unusual but experimentally verifiable consequences. Our analysis is based on a recently proposed model,<sup>1</sup> which—by introducing electronic correlations, and a *linear* coupling between electrons and phonons (as determined in frozen-phonon local-density calculations,<sup>3</sup> for example)—results in a *dynamic* “double-well” structure describing oscillations between two dominant Cu(1)-O(4) bond lengths. This structure is similar to that inferred in x-ray-absorption fine-structure (XAFS) studies of  $\text{YBa}_2\text{Cu}_3\text{O}_7$  and  $\text{TlBa}_2\text{Ca}_3\text{Cu}_4\text{O}_{11}$ ,<sup>4</sup> and pair-distribution-function analysis of neutron-scattering data in, e.g.,  $\text{Tl}_2\text{Ba}_2\text{CaCu}_2\text{O}_8$ .<sup>5</sup> Below, we shall show that such a polaron approach can also account for some of the observed optical anomalies both in Raman scattering<sup>6</sup> and in infrared spectra.<sup>7</sup> Furthermore, inelastic neutron-scattering resolution<sup>8</sup> is now approaching the regime where it is possible to probe relevant local dynamics for this polaron tunneling.

While conventional local-density methods provide useful information on high- $T_c$  materials—for example, estimating parameter values in an effective many-body Hamiltonian—strong electronic correlation effects, together with the nonadiabatic, local charge-distribution character of the problem, renders these approaches inappropriate for our purposes. This is clearly demonstrated by recent calculations<sup>9</sup> which find lattice-polaron states in strongly correlated electronic models with moderate strength electron-lattice coupling. However, even these calculations are inadequate if relevant electronic and

phonon degrees of freedom have similar time scales and/or the system size is small, as for the problem here. We have therefore used a numerically exact diagonalization technique.<sup>1</sup>

Our main results are the following. (i) The predictions of the nonlinear and nonadiabatic dynamics of the cluster are consistent with both structural and optical data. (ii) The usefulness of energy-resolved pair-distribution functions is shown, suggesting specific analysis of inelastic neutron scattering to investigate the predictions of this model. (iii) A Raman-active state close in energy to the in-plane “330- $\text{cm}^{-1}$ ” buckling mode is predicted. A coupling between these two states may have important consequences for the physics of  $\text{YBa}_2\text{Cu}_3\text{O}_7$ .

We assume that the dynamics of the O(4)-Cu(1)-O(4) cluster can be effectively separated from the rest of the lattice. We make this approximation because the dynamic coupling to the planes is weak due to the long bond lengths, and because some aspects of the coupling along the chain direction can be taken into account by an effective Hamiltonian by integrating out the degrees of freedom associated with the chain oxygens O(1). Including the nearest-neighbor Coulomb interactions, we arrive at the cluster Hamiltonian,

$$H = H_{\text{el}} + H_{\text{el-ph}} + H_{\text{ph}}, \quad (1)$$

where

$$H_{\text{el}} = \sum_n \epsilon_n \rho_n - \sum_{\langle nn' \rangle \sigma} t_{nn'} (c_{n\sigma}^\dagger c_{n'\sigma} + \text{H.c.})$$

$$+ U \sum_n \rho_{n\uparrow} \rho_{n\downarrow} + \sum_{\langle nn' \rangle} V_{nn'} \rho_n \rho_{n'},$$

$$H_{\text{el-ph}} = \lambda_{\text{IR}} (a_{\text{IR}} + a_{\text{IR}}^\dagger) (\rho_3 - \rho_1)$$

$$+ \lambda_{\text{R}} (a_{\text{R}} + a_{\text{R}}^\dagger) (\rho_1 + \rho_3 - s_0),$$

$$H_{\text{ph}} = \hbar \omega_{\text{IR}} a_{\text{IR}}^\dagger a_{\text{IR}} + \hbar \omega_{\text{R}} a_{\text{R}}^\dagger a_{\text{R}}.$$

This is similar to the Hamiltonian introduced in Ref. 1. In Eq. (1),  $c_{n\sigma}^\dagger$  creates a hole of spin  $\sigma$  at site  $n$ ,

$\rho_{n\sigma} = c_{n\sigma}^\dagger c_{n\sigma}$ , and  $\rho_n = \sum_{\sigma} \rho_{n\sigma}$ . Here,  $n = 1, 3$  denote the axial O(4) sites and  $n = 2$  is the chain Cu(1) site. The notation  $\langle nn' \rangle$  refers to the bonds:  $t_{nn'} = t$  for the hopping matrix elements between the O(4) and Cu(1) sites and  $t'_{nn'} = t'$  for the effective matrix element between the O(4) sites. The parameter  $s_0$  is chosen to avoid any artificial shrinkage of the cluster, allowing the use of a reduced basis set. The isolated three-site cluster has two phonon modes for displacements in the  $z$  direction that do not change the center of mass. These bare modes are assumed to be harmonic. The symmetric phonon mode is Raman active and the antisymmetric one is infrared active. They are described by boson operators  $a_R$  and  $a_{IR}$  with bare frequencies  $\omega_R$  and  $\omega_{IR}$ , respectively.

The parameters in  $H_{el}$  are taken as  $\epsilon_{1,3} = 0.307$  eV,  $\epsilon_2 = -\epsilon_{1,3}$ ,  $t = 0.634$  eV,  $U = 4.44$  eV,  $V_{nn'} = 0$ , which are representative values, guided by local-density calculations.<sup>3</sup> We estimate  $t' \sim t/10$ . For bare phonon energies, we choose  $\hbar\omega_{IR} = 59.3$  meV and  $\hbar\omega_R = 71.5$  meV. The electron-phonon coupling constants,  $\lambda_{IR}$  and  $\lambda_R$ , are varied so that the XAFS experiments and optical data can be simultaneously reconciled with the model's predictions; see below.<sup>10</sup>

We assume two holes within the O(4)-Cu(1)-O(4) cluster.<sup>1</sup> In the ground state, one hole is predominantly located at the Cu(1) site while the other fluctuates between the O(4) sites, in agreement with core-level x-ray-absorption measurements implying excess holes located in the O(4)  $2p_z$  orbitals.<sup>11</sup> Both spin-0 and spin-1 states are considered.

As was found in Ref. 1, sufficiently large values of  $\lambda_{IR}$  dynamically generate a length scale,  $\delta l$ , associated with a dynamic double-well structure in the infrared distortion. In this regime, the motion of the phonons is strongly correlated with the hole motion, corresponding to polaron tunneling.<sup>1</sup> Despite the generalizations introduced in the Hamiltonian, Eq. (1), a similar picture emerges. Moreover, as the system moves from weak coupling to strong coupling, the Raman active states show pronounced minima in the intermediate region, whereas the infrared active states decrease in a regular fashion; see Fig. 1. Interestingly, the location of the minima is close to the value of  $\lambda_{IR}$  where the double-well structure begins to develop and where the dynamics of the system becomes highly nonlinear and nonadiabatic. Assuming that the parameters in the model depend on temperature, this nonmonotonic behavior might explain the experimental observation that the Raman active state at  $\sim 500$   $\text{cm}^{-1}$  softens<sup>6</sup> whereas the infrared active state at  $\sim 580$   $\text{cm}^{-1}$  hardens<sup>7</sup> as the temperature is decreased from 100 to 50 K. It is also possible that the above behavior implies the weakening or suppression of the double well due to renormalization of the electron-phonon coupling constants by superconducting fluctuations. However, these suggestions remain speculative in absence of a specific microscopic coupling of the cluster to its environment and, in particular, to the  $\text{CuO}_2$  planes which predominantly carry the superconductivity.

We find that  $\lambda_{IR} = 0.143$  eV and  $\lambda_R = 0.260$  eV (and other parameter values as defined above) lead to reasonable agreement with experiments. Choosing  $s_0 = 1.18$ ,

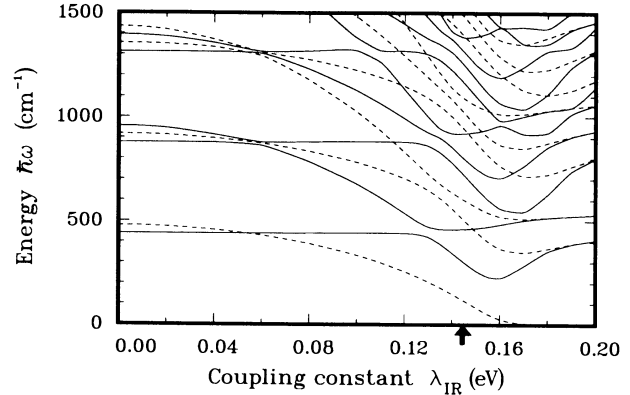


FIG. 1. The energy spectrum relative to the ground state of the O(4)-Cu(1)-O(4) cluster as a function of  $\lambda_{IR}$  with fixed  $\lambda_R = 0.260$  eV. The Raman and infrared active states are shown as solid and dashed lines, respectively. The arrow indicates the experimentally optimal value of  $\lambda_{IR}$  (0.143 eV).

the size of the cluster is not changed by the electron-phonon interactions. First, the Cu(1)-O(4) bond-length splitting  $\delta l$  is 0.11 Å which approximately equals the XAFS result.<sup>4</sup> Second, a doublet of infrared active states at frequencies 526 and 614  $\text{cm}^{-1}$  is predicted in the experimentally relevant region  $\sim 580$   $\text{cm}^{-1}$  where a broad shoulder is observed<sup>12</sup> below the main infrared peak; see Fig. 2. The 526- $\text{cm}^{-1}$  state is a complicated multiphonon state involving the infrared degree of freedom whereas the 614- $\text{cm}^{-1}$  state contains basically two bare infrared phonons and one bare Raman phonon.

The predicted infrared and Raman spectra exhibit several additional interesting features: (i) The lowest-energy peak in the infrared absorption occurs at the polaron tunneling energy  $\hbar\omega_T \simeq 127$   $\text{cm}^{-1}$ . (ii) The lowest-energy features in the Raman spectrum are located at 317 and 460  $\text{cm}^{-1}$  of which the first is highly nonlinear in terms of bare phonon degrees of freedom, whereas the second is only a weakly renormalized bare one-Raman

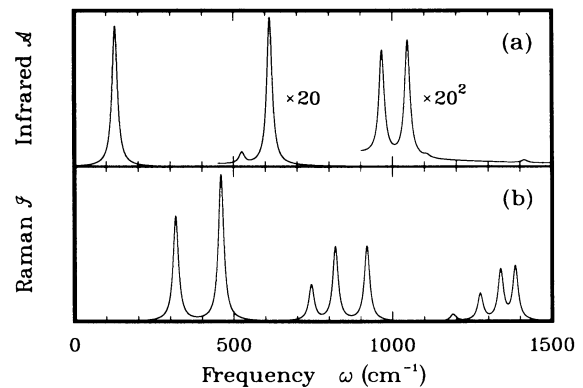


FIG. 2. (a) The infrared absorption and (b) the Raman scattering spectrum (in arbitrary units) with  $\lambda_{IR} = 0.143$  eV and  $\lambda_R = 0.260$  eV (the double-well regime) at zero temperature. The Raman spectrum is calculated at the incident photon energy of 2.5 eV. The infrared spectrum is scaled up by a factor of 20 above 450  $\text{cm}^{-1}$  and by a factor of 20<sup>2</sup> above 900  $\text{cm}^{-1}$ . A Lorentzian broadening of resonances with full width at half maximum of 20  $\text{cm}^{-1}$  has been included by hand.

phonon state observed experimentally at  $\sim 500 \text{ cm}^{-1}$ . (iii) There is a clear progression of Raman active states in intervals of  $\sim 450 \text{ cm}^{-1}$ , some of which are close in energy to the unassigned state at  $\sim 700 \text{ cm}^{-1}$ , observed by inelastic neutron scattering.<sup>8(a)</sup> In particular, the state at  $744 \text{ cm}^{-1}$  has multiphonon character and is therefore inaccessible to simple lattice dynamics.

The  $317\text{-cm}^{-1}$  Raman active state is a robust consequence of the model and offers the intriguing possibility that the in-plane “ $330\text{-cm}^{-1}$ ” buckling mode is coupled to the O(4) motion and that the cluster is driving an in-plane phonon—the “ $330\text{-cm}^{-1}$ ” mode is observed to be anomalous in its shape and temperature dependence.<sup>6,13</sup> Indeed, recent local-density calculations<sup>14</sup> imply an admixture of O(4) and in-plane oxygen degrees of freedom. Such mixing of states makes a small-cluster calculation for Raman intensities unreliable because we have to consider the full unit cell. It is also shown experimentally that the O(4) mode couples to electronic degrees of freedom in the plane.<sup>15</sup>

The polaron-tunneling model predicts a strong infrared-active state at  $\hbar\omega_T$  that has not been directly observed; other absorptions in this region may hamper its detection. It may be also that much of the oscillator strength has been shifted down to much lower energies by local disorder and inhomogeneity.<sup>8</sup> Details of the effect of diagonal and off-diagonal disorder, as well as temperature will be given elsewhere.<sup>16</sup>

There are probes preferable to optical response for measuring local, dynamical effects. One is XAFS,<sup>4</sup> which is able to probe instantaneous local structure by studying changes at high-momentum transfer. Another is inelastic neutron scattering which measures the dynamic structure factor  $S(q, \omega)$ : indeed, recent time-of-flight experiments<sup>8</sup> on high- $T_c$  materials have demonstrated its usefulness for detecting changes at short-length scales and slow time scales. Below, we describe signatures of the polaron-tunneling behavior which may be most important in resolving the nature of the double-well Cu(1)-O(4) bond-length distribution inferred in XAFS studies.

Inelastic neutron scattering measures the dynamic structure factor:<sup>17</sup>

$$S(q, \omega) = \sum_{nn'} v_{nn'} \int_{-\infty}^{\infty} \frac{dt}{2\pi} e^{-i\omega t} \langle e^{-iqr_n(0)} e^{iqr_n(t)} \rangle, \quad (2)$$

where  $r_n(t)$  is the position operator of the  $n$ th scattering nucleus in the Heisenberg picture<sup>18</sup> and  $v_{nn'}$  is a cross-section coefficient determined by the scattering lengths of individual nuclei.<sup>19</sup>  $S(q, \omega)$  for our cluster is a sum of delta functions in  $\omega$  at the same frequencies as the infrared or Raman lines; the intensity of each line varies with  $q$  (momentum transfer along the  $z$  axis). The results are summarized in Fig. 3 which shows  $S(q, \omega)$  and its spatial Fourier transform  $S(r, \omega)$  for various values of energy transfer  $\hbar\omega$  at zero temperature. As described below, these results illustrate important manifestations of dynamic polaron tunneling (multiphonon, nonlinear, and nonadiabatic effects) which no harmonic phonon theory can produce. The features also appear in the static structure factor  $S(q, t=0)$  and in its dynamic counterparts, where the integration is made only over some limited

range of frequencies.<sup>8</sup>

The state at  $\hbar\omega_T$  has large intensity which emphasizes the significance of the slow time scale of the polaron tunneling; see Fig. 3(a). Small wavelength oscillatory behavior in  $S(q, \omega_T)$  as a function of  $q$  is evidence of the length scale  $\delta l$  associated with the double well. Note that the larger wavelength oscillations, with the periods  $2\pi/l_0$  and  $\pi/l_0$ , are due to the mean Cu(1)-O(4) and O(4)-O(4) bond lengths,  $l_0$  and  $2l_0$  ( $l_0 = 1.87 \text{ \AA}$  in  $\text{YBa}_2\text{Cu}_3\text{O}_7$ ). Moreover, the envelope of these oscillations—given by the coherent part of the dynamic structure factor—as well as the smooth background—partially due to the incoherent contribution—vary in a nonuniform way. This differs from a harmonic Debye-Waller factor of the symmetric cluster: since the Debye-Waller factor describes the effect of the quantum fluctuations, it also contains information about the tunneling behavior.

Our results demonstrate that the elastic scattering, given by  $S(r, \omega=0)$  (not shown), contains no clear signature of the Cu(1)-O(4) bond-length splitting while the static structure factor (pair-distribution function)  $S(r, t=0)$  (not shown) may yield only marginal evidence for it—in fact, in the present case, quantum lattice fluctuations are too large compared to the length scale,  $\delta l \approx 0.11 \text{ \AA}$ , so that it cannot be detected conclusively by

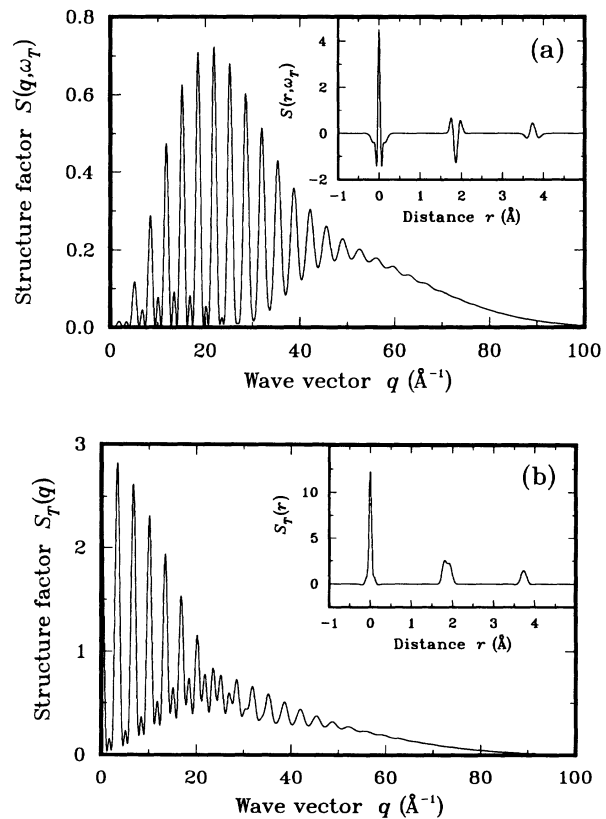


FIG. 3. The dynamic structure factors (a)  $S(q, \omega_T)$ , and (b)  $S_T(q) \equiv \int_0^{\omega_T} d\omega S(q, \omega)$ , as a function of momentum transfer  $\hbar q$ . The insets show corresponding Fourier transforms (in units of  $\text{\AA}^{-1}$ ) as a function of distance  $r$ . The parameters are  $\lambda_{\text{IR}} = 0.143 \text{ eV}$  and  $\lambda_{\text{R}} = 0.260 \text{ eV}$  (i.e., in the experimentally relevant double-well regime).

these conventional correlation functions. In contrast,  $\delta l$  can be approximately resolved if only the frequency components up to the relevant time scale of the problem—i.e., the tunneling time  $1/\omega_T$ —are included. This is shown in Fig. 3(b) which displays a double peak around 1.87 Å, the splitting being 0.09 Å. For large  $\delta l$ , the splitting can be resolved by  $S(r, t=0)$  while  $S(r, \omega=0)$  will still not show any clear signature, in agreement with experimental observations (cf. Fig. 2 in Ref. 5).

We emphasize that oxygen locations cannot all be determined by high-frequency dynamic structure factors;<sup>20</sup> the Cu(1)-O(4) bond-length splitting here is most sensitive to a low-frequency dynamic-structure-factor analysis. Most notably, we predict—as a signature of the slow time scale—an anomalously large dynamic structure factor at  $\hbar\omega_T$  which leads to an intensity increasing rapidly with  $q$  at small momentum transfer. Moreover, a length scale  $\delta l$  appears which generates an additional  $q$

period. These modulations should be accessible in measurements of  $\int_0^{\omega_T} d\omega S(q, \omega)$ , which appears to be the optimal quantity to be probed.

In conclusion, we have shown that a polaron-tunneling model leads to structural results consistent with XAFS and neutron-scattering data, and an excitation spectrum compatible with available optical data. In addition, this model predicts unusual nonlinear, nonadiabatic features which should be verifiable by inelastic neutron-scattering and optical spectroscopy studies. Finally, we noted an important implication that the in-plane buckling mode and the O(4)-Cu(1)-O(4) cluster state around  $330 \text{ cm}^{-1}$  may be coupled.

It is our pleasure to thank S. Billinge, S. Conradson, and M. Arai for helpful discussions, and T. Timusk for providing his infrared data prior to publication. This work was supported by the U.S. Department of Energy.

<sup>1</sup>J. Mustre de Leon *et al.*, Phys. Rev. Lett. **68**, 3236 (1992).

<sup>2</sup>J. Ranninger and U. Thibblin, Phys. Rev. B **45**, 7730 (1992).

<sup>3</sup>W. Pickett, Rev. Mod. Phys. **61**, 433 (1989).

<sup>4</sup>S. Conradson *et al.*, Science **248**, 1394 (1990); J. Mustre de Leon *et al.*, Phys. Rev. Lett. **65**, 1675 (1990); R. Allen *et al.*, Phys. Rev. B **44**, 9480 (1991).

<sup>5</sup>T. Egami *et al.*, Physica C **185-191**, 867 (1991).

<sup>6</sup>E. Altendorf *et al.*, Physica C **175**, 44 (1991).

<sup>7</sup>H. Obhi and E. Salje, Physica C **171**, 547 (1990).

<sup>8</sup>(a) M. Arai *et al.*, Phys. Rev. Lett. **69**, 359 (1992); (b) M. Arai *et al.* (unpublished).

<sup>9</sup>For example, see V. Anisimov *et al.*, Phys. Rev. Lett. **68**, 345 (1992), and references therein.

<sup>10</sup>Despite the apparently large number of parameters, we find that only a few of them are significantly independent.

<sup>11</sup>A. Bianconi *et al.*, Phys. Rev. B **38**, 7196 (1988); C. T. Chen *et al.*, Phys. Rev. Lett. **68**, 2543 (1992).

<sup>12</sup>M. Bauer, Ph.D. Thesis, Tübingen, 1990; D. Bonn *et al.*, Phys. Rev. **37**, 1574 (1988); T. Timusk (private communication).

<sup>13</sup>For example, see S. Cooper and M. Klein, Comments Condens. Matter Phys. **15**, 99 (1990).

<sup>14</sup>C. Rodriguez *et al.*, Phys. Rev. B **42**, 2692 (1990); R. Cohen, W. Pickett, and H. Krakauer, Phys. Rev. Lett. **64**, 2575

(1990).

<sup>15</sup>M. Reedyk and T. Timusk, Phys. Rev. Lett. **69**, 2705 (1992); J. Nickel, D. Morris, and J. Ager III, *ibid.* **70**, 81 (1993); H. Krakauer (private communication).

<sup>16</sup>M. Spicci, M. Salkola, and A. Bishop (unpublished).

<sup>17</sup>S. Lovesey, *Theory of Neutron Scattering from Condensed Matter* (Clarendon, Oxford, 1984), Vol. I. We include the cross sections of individual nuclei in the definition of  $S(q, \omega)$ . [Note that, in the text, by  $S(q, \omega)$  we mean  $\int_{\omega-\delta}^{\omega+\delta} d\omega' S(q, \omega')$ ,  $\delta=0^+$ .]

<sup>18</sup>These operators,  $r_n \equiv r_n^{(0)} + z_n$ , are related to the oxygen and copper coordinates,  $z_n$  ( $n=1, 2, 3$ ), measured from the average positions  $r_n^{(0)}$ , so that  $u_{\text{IR}} = (z_1 - 2z_2 + z_3)/\sqrt{3}$  and  $u_{\text{R}} = (z_1 - z_3)/\sqrt{2}$ , where the phonon coordinates are  $u_{\text{IR}} = \sqrt{\hbar/2m_{\text{O}}\omega_{\text{IR}}}(a_{\text{IR}} + a_{\text{IR}}^\dagger)$  and  $u_{\text{R}} = \sqrt{\hbar/2m_{\text{O}}\omega_{\text{R}}}(a_{\text{R}} + a_{\text{R}}^\dagger)$ . We have taken the ratio of the effective copper to oxygen masses  $m_{\text{Cu}}/m_{\text{O}} \simeq 4$ .

<sup>19</sup>The coefficients  $v_{nn'}$  are normalized so that  $\sum_n v_{nn} = 1$ ; their relative values are taken from Ref. 17.

<sup>20</sup>However, Ref. 8(a) suggests some evidence for local structural anomalies, similar to those found in studying (Ref. 5) the static pair-correlation factor, but using high-frequency dynamic structure factors as probes.